Reduction of the energy loss of swift molecular ions in solids due to vicinage effects in the charge state

Santiago Heredia-Avalos and Rafael Garcia-Molina

Departamento de Física, CIOyN, Universidad de Murcia, Apartado 4021, E-30080 Murcia, Spain

We have calculated the energy loss of swift O_2^+, N_2^+, and C_n^+ ($n=2-60$) molecular ions moving through an amorphous carbon target. The dielectric formalism is used to evaluate the vicinage effects in the energy loss of the atomic ions that form the molecular projectile, but we take into account that the charge state of these atomic ions is affected by their correlated motion through the target and by the screened Coulomb potential between them. When vicinage effects in the charge state are taken into account, the Coulomb repulsion is weakened, leading to a reduction in the interatomic separations ($\sim 3\%$ for N_2^+ and $\sim 9\%$ for C_{60}^+, both having similar velocities). These charge state effects can be neglected for diatomic molecular ions, but they give rise to a reduction of $\sim 8\%$ in the vicinage effects in the energy loss of larger molecular ions with cagelike geometrical structures, like C_n^+ ($n=20,60$) projectiles.

PACS number(s): 34.50.Bw, 36.40.−c, 61.48.+c

I. INTRODUCTION

Molecular beams interacting with solids are used for both basic and applied purposes. In the former case, one can go deeply into the study of the processes that take place when charged particles move through matter, and in the latter case, new methods to modify the structure of a material can be accomplished. The pioneering work by Brandt *et al.* [1] clearly showed experimentally and theoretically that the energy loss per atom of swift molecular ions was different from that of isolated atomic ions of the same element with identical velocity. These differences were attributed to the correlated motion of the molecular constituents through the target, in such a manner that vicinage (or interference) effects appear among the particles in motion, due to the proximity of the electronic excitations they induce in the stopping medium. This vicinage effect in the energy loss can be properly described in terms of the wake potential [2] that each projectile induces in the solid, which produces electronic perturbations whose intensity oscillates but rapidly decreases when the distance to the projectile increases; these perturbations are located in practice in a cone-shaped region that extends mainly in the rear part of the moving projectile.

After Ref. [1] many other works were published, extending that study [3–14] and even discussing other consequences of the vicinage effects [15,16]. The interested reader can consult the recent reviews by Arista [17] and by Mišković *et al.* [18] on the energy loss of swift molecular ions in solids.

Our aim in this paper is to study the energy loss of swift molecular ions, taking into account that the proximity of the molecular fragments in correlated motion also affects their charge state. This vicinage effect reduces the charge state of the fragments as compared to atomic ions [19–21]; in consequence, there is a less pronounced Coulomb repulsion between these fragments. The combination of this closer proximity and the different energy loss of the molecular fragments due to their reduced charge states will affect the energy loss of the whole molecular projectile.

In what follows we briefly introduce the model we use in Sec. II and discuss our results in Sec. III; finally, we present our conclusions in Sec. IV. Atomic units will be used throughout this work except where otherwise stated.

II. MODEL

When a swift X_n^+ molecular ion moves through a solid target, it loses its binding electrons in the first atomic layers. The n atomic ions resulting from the dissociation of the molecular ion undergo electronic loss and capture processes until they acquire an average charge state due to a dynamical equilibrium between all possible charge states. This average charge state is different from the average charge state for an isolated atomic ion, depending on both the nature and the geometrical structure of the molecular ion; this phenomenon is called the vicinage effect in the charge state. In order to take these effects into account, we use a model [21] that provides a self-consistent method to evaluate the average charge state of the atomic ions that constitute the molecular ion, for a given geometrical structure. In this model the average number of electrons bound to the i molecular fragment, $\langle N_i^* \rangle$, is evaluated through [21]

$$\langle N_i^* \rangle = \mathcal{Z}_i \exp\left(\frac{-0.92 \ v_r}{\mathcal{Z}_i^{2/3}} \right), \qquad (1)$$

v_r being the relative velocity of the i fragment with respect to the valence electrons of the target [22]. $\mathcal{Z}_i$ is the effective nuclear charge of the fragment, which depends on both the number and the relative position of the rest of the neighboring fragments,

$$\mathcal{Z}_i = Z_i + \sum_{j \neq i}^{n} (Z_j - \langle N_j^* \rangle) \frac{\langle r_i \rangle}{R_{ij}} \exp\left(-\frac{R_{ij}}{a} \right), \qquad (2)$$

where Z_i is the atomic number of the i fragment, R_{ij} is the interatomic distance between a pair of molecular fragments, $\langle r_i \rangle$ is the mean electronic radius of the i fragment, and $a = [v^2/\omega_p^2 + v_F^2/(3\omega_p^2)]^{1/2}$ is the screening length [21]; in our case $\omega_p = 0.86$ a.u. is the plasmon energy for amorphous carbon and $v_F = 1.2$ a.u. is the corresponding Fermi velocity. In

order to evaluate $\langle r_i \rangle$, we use the Brandt-Kitagawa model [23],

$$\langle r_i \rangle = \frac{0.96 \langle N_i \rangle^{2/3}}{Z_i - \langle N_i \rangle / 7}, \tag{3}$$

where $\langle N_i \rangle$ is the average number of electrons bound to the isolated atomic ion, which is obtained by substituting $\mathcal{Z}_i$ by Z_i in Eq. (1).

Equations (1) and (2) constitute a system of $2n$ coupled nonlinear equations, which must be solved numerically. This provides a self-consistent method to evaluate the average charge state of all the fragments of a molecular ion, i.e., $Q_i = Z_i - \langle N_i^* \rangle$. As the values of R_{ij} change with time due to the Coulomb repulsion, the value of the average charge state of each fragment will also be a function of the time (in addition to its dependence on the nature of the stopping medium and on the projectile velocity and geometry).

Note that for an atomic ion $\mathcal{Z} = Z$, and Eq. (1) results in the well-known expression provided by Ziegler *et al.* in Ref. [22], which gives good agreement with the experimental data.

To obtain the evolution with time of the interatomic distance between the dissociated fragments, we solve numerically the set of coupled Newton equations for these atomic ions, considering the vicinage effects in the charge state and that the ions interact through a screened Coulomb potential. For a pair of atomic ions separated by the interatomic distance R_{ij}, this potential is given by

$$V(R_{ij}) = \frac{Q_i Q_j}{R_{ij}} \exp\left(-\frac{R_{ij}}{a}\right). \tag{4}$$

It should be kept in mind that the values of Q_i and R_{ij} are obtained sequentially in such a manner that the values of R_{ij} determine those of Q_i and vice versa.

In Fig. 1 we depict the normalized interatomic distance as a function of the time t inside the target, for the case of (a) O_2^+ and (b) N_2^+ molecular ions moving through amorphous carbon foils; $R_{12}^0 = 2.11$ a.u. is the initial interatomic distance for both diatomic molecular ions [24]. The solid lines correspond to calculations done when the vicinage effects in the charge state are considered, whereas the dashed lines represent the results obtained when they are not taken into account, so $\langle N_i^* \rangle = \langle N_i \rangle$. The numbered labels indicate the projectile energy (in MeV/atom). Such energies correspond to those used in the experiments reported by Steuer *et al.* [4]. As expected, when the projectiles are more energetic the average charge state increases and the screening is less important, so they separate more quickly. In addition, considering vicinage effects in the charge state provides a weaker Coulomb repulsion between the fragments, due to the reduction in their charge state. All the same, note that the observed differences in the Coulomb repulsion when the vicinage effects in the charge state are included (or not) are very small; for instance, the interatomic distance is reduced ~3% for N_2^+ ions with $E = 500$ keV/atom at $t \sim 40$ fs. These differences are more sizable when larger molecular projectiles are considered, such as C_{60}^+ molecular ions. We assume that the geometrical structure of the C_{60}^+ molecular ion is the same
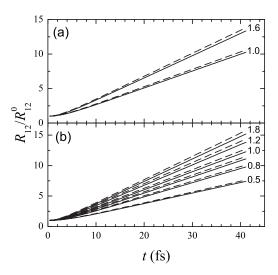

FIG. 1. Normalized interatomic distances as a function of the time t inside the target, when vicinage effects in the charge state are considered (solid line) or not (dashed line), for the case of (a) O_2^+ and (b) N_2^+ incident on amorphous carbon foils. The numbered labels indicate the projectile energy in MeV/atom and $R_{12}^0 = 2.11$ a.u. is the initial interatomic distance for both N_2^+ and O_2^+ molecular ions [24].

as that of the C_{60} neutral molecule, which has a cagelike structure with only two different interatomic distances between first neighbors: $R_{12}^0 = 2.63$ a.u. and $R_{13}^0 = 2.74$ a.u. [25]. We depict in Fig. 2 the normalized interatomic distances as a function of time for the case of C_{60}^+ molecular ions incident on amorphous carbon foils with $E = 0.455$ MeV/atom, which corresponds to one of the experimental situations analyzed by Baudin *et al.* [6]; in this case
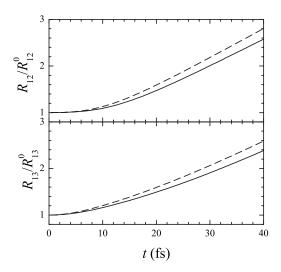

FIG. 2. Normalized interatomic distances as a function of the time t inside the target, when vicinage effects in the charge state are considered (solid line) or not (dashed line), for the case of C_{60}^+ incident with $E = 0.455$ MeV/atom on an amorphous carbon target; $R_{12}^0 = 2.63$ a.u. and $R_{13}^0 = 2.74$ a.u. are the only two different initial interatomic distances between first neighbors of a C_{60} molecule [25].
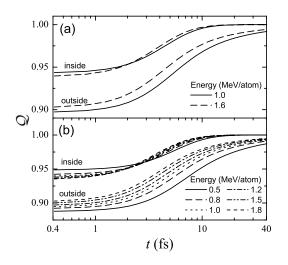
FIG. 3. Charge state ratio as a function of the time t for (a) O_2^+ and (b) N_2^+ moving inside an amorphous carbon target; the charge state ratio outside the target is also represented. Different types of lines correspond to the projectile energies indicated in the figure.

FIG. 4. Charge state ratio as a function of the time t for C_{60}^+ moving inside an amorphous carbon target; the charge ratio outside the target is also represented. Different types of lines correspond to the projectile energies indicated in the figure.

the interatomic distances are reduced ~9% at $t \sim 40$ fs.

It is worth mentioning that the experimental charge state ratio, which can be measured when the atomic ions exit the target, is different from the average charge state ratio our model uses inside the foil. We consider that, just after each fragment exits the foil, no further changes in the charge state will take place while the ions travel in vacuum until they reach the detector; the atomic ion that exits the foil in the ℓth place acquires its average charge state under the influence of the remaining $(n-\ell)$ neighbors, screened by the electrons of the solid target, plus the unscreened effect of the $(\ell-1)$ neighbors in the vacuum [i.e., with $a=\infty$ in Eq. (2)]. Summarizing, vicinage effects change abruptly when the ion emerges from the target due to the sudden disappearance of screening by the target electrons.

To quantify the vicinage effects on the charge state inside the solid, we use the average charge state ratio, which is defined as

$$\mathcal{Q} = \frac{\sum\limits_{i=1}^{n} (Z_i - \langle N_i^* \rangle)}{\sum\limits_{i-1}^{n} (Z_i - \langle N_i \rangle)}. \tag{5}$$

Note that, according to our model, the average charge state ratio inside the target is different from that just after the atomic ions leave the foil. In the following, we refer to the latter as the $\mathcal{Q}$ outside the target, in contrast to $\mathcal{Q}$ inside the target, which cannot be measured.

Figure 3 shows the variation of the average charge state ratio as a function of the time (a) for O_2^+ and (b) for N_2^+ molecular ions moving through amorphous carbon at different projectile energies (indicated in MeV/atom). The curves labeled "inside" represent the average charge state ratio when the atomic ions move inside the target after an elapsed
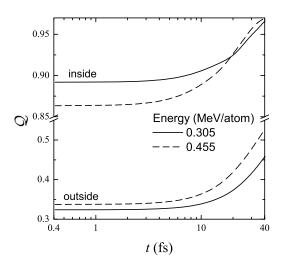
time t, whereas the curves labeled "outside" represent the average charge state ratio just when the atomic ions emerge from the target after a dwell time t, but taking into account the previous motion of each ion inside the target. As expected, the average charge state ratio both inside and outside the target is smaller than 1 for short times, but it tends to 1 as the time increases. In addition, the vicinage effects in the charge states are more important outside than inside the target. In the latter case all the fragments interact among themselves through a screened potential, whereas in the former some of the fragments can interact with an unscreened potential, giving rise to a stronger vicinage effect. On the other hand, Fig. 3 shows that the charge ratio inside the target remains almost constant although the projectile energy varies strongly; however, the charge state ratio outside the target clearly changes, increasing as the projectile energy increases; that is, the vicinage effects in the charge state decrease when the projectile energy increases.

The differences between $\mathcal{Q}$ inside and outside the target become more remarkable as the size of the molecular projectile increases, which is clearly observed in Fig. 4, where we depict the average charge state ratio for C_{60}^+ ions moving through (or after leaving) an amorphous carbon foil. Vicinage effects in the charge state are drastically reduced inside the target because the interaction between all the fragments is screened by the target electrons.

In order to calculate the electronic energy loss of the atomic ions dissociated from a molecular projectile, we use the dielectric formalism. The stopping power ratio, which is defined as the ratio between the stopping power of the target for a molecular projectile and that for the individual atomic ions with the same velocity, is a useful quantity to evaluate the vicinage effects in the energy loss. In this scheme, the instantaneous stopping power ratio for an X_n^+ molecular ion that travels with velocity v through a target is given by [26]

$$\mathcal{R} = \frac{S_p(X_n^+)}{nS_p(X^+)} = 1 + \frac{2}{n}\sum_{i=1}^{n-1}\sum_{j>i}^{n} I(R_{ij}, \psi_{ij}), \qquad (6)$$

where $I(R_{ij}, \psi_{ij})$ is an interference function that takes into account the spatial correlation between the i and j fragments separated by the interatomic distance R_{ij} and with their internuclear axis forming an angle ψ_{ij} in relation to the beam direction. $S_p(X_n^+)$ and $S_p(X^+)$ are the stopping powers of the target for the molecular projectile and the individual atoms, respectively. The previous equation arises from a superposition of undisturbed wake potentials for the individual fragments.

From an experimental point of view, there are two interesting values of the interference function for a homonuclear molecular projectile: (i) when its orientation is random with respect to the beam direction,

$$\langle I(R_{ij})\rangle = \frac{2}{\pi v^2 S_p}\int_0^\infty dk \frac{[\rho_i(k)]^2}{k}$$
$$\times \int_0^{kv} d\omega\, \omega \frac{\sin(kR_{ij})}{kR_{ij}}\mathrm{Im}\left(\frac{-1}{\varepsilon(k,\omega)}\right), \qquad (7)$$

which is obtained taking an average over all the angular orientations, and (ii) for a linear molecular projectile ($\psi_{ij}=0$) that crosses the solid with its interatomic axis aligned with respect to the beam direction,

$$I(R_{ij}) = \frac{2}{\pi v^2 S_p}\int_0^\infty dk \frac{[\rho_i(k)]^2}{k}$$
$$\times \int_0^{kv} d\omega\, \omega \cos\left(\frac{\omega R_{ij}}{v}\right)\mathrm{Im}\left(\frac{-1}{\varepsilon(k,\omega)}\right). \qquad (8)$$

where $\mathrm{Im}[-1/\varepsilon(k,\omega)]$ is the target energy-loss function, which is a function of the momentum k and energy ω transferred to the target electrons, and it is modeled as described in Refs. [27,28], i.e., by a linear combination of Mermin-type energy-loss functions that characterize the response of valence-band electrons, together with generalized oscillator strengths to take into account the ionization of K-shell electrons. $\rho_i(k)$ is the Fourier transform of the charge density corresponding to the i fragment, which is obtained by means of [23]

$$\rho_i(k) = \langle N_i^* \rangle\left[1 + k^2\left(\frac{0.23\langle N_i^*\rangle^{4/3}}{(Z_i - \langle N_i^*\rangle/7)^2}\right)\right]^{-1}. \qquad (9)$$

In Eqs. (7) and (8), S_p is the stopping power of the target for the isolated X^+ atomic ion, which is evaluated through

$$S_p = \frac{2}{\pi v^2}\int_0^\infty dk \frac{[\rho_i(k)]^2}{k}\int_0^{kv} d\omega\, \omega\, \mathrm{Im}\left(\frac{-1}{\varepsilon(k,\omega)}\right). \quad (10)$$

Equations (7), (8), and (10) are based on the dielectric formalism, so they assume a linear response of the medium to the external perturbation produced by the passing ions. The dielectric formalism loses validity as the perturbation grows, i.e., when the projectile has high charge and low energy. This is especially relevant when evaluating S_p, because
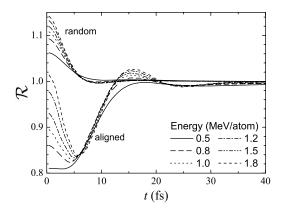

FIG. 5. Instantaneous stopping power ratio for N_2^+ molecular projectiles when moving through an amorphous carbon foil with several energies (corresponding to different line types) as a function of time; vicinage effects in the charge state were taken into account in the calculations.

the stopping power is calculated from the self-induced potential in the target just at the position of the atomic ion, where the highest perturbation is produced. In this situation nonlinear effects, such as the Bloch correction [29], become more significant, reducing the total stopping power near the maximum. Equation (10) does not include the stopping power due to projectile excitation (although it can be neglected according to Ref. [30]) or the electronic capture and loss by the projectile, which can increase the value of the total stopping power near the maximum. As the numerator and denominator have been determined using the same theoretical basis (i.e., ignoring the Bloch correction, projectile excitation, and electronic capture and loss by the projectile) and the vicinage effects in the charge state are so small, a more accurate estimate of these effects is not relevant at this stage.

Figure 5 shows the instantaneous stopping power ratio, evaluated according to Eq. (6), and Eq. (7) or (8), depending on the projectile orientation, for N_2^+ molecular projectiles when moving through an amorphous carbon foil with several energies. It is worth noticing that $\mathcal{R}$ is always greater than 1 for randomly oriented projectiles, whereas it is in most cases lower than 1 for aligned ones. Moreover, when the projectile energy is increased, greater vicinage effects ($\mathcal{R}$ separates from 1) are obtained for randomly oriented projectiles, but the opposite tendency appears for aligned projectiles, i.e., there are smaller vicinage effects ($\mathcal{R}$ approaches 1) in the energy loss as the projectile energy increases.

These vicinage effects are sizable for only a short time ($t \lesssim 5$ fs), due to the closeness of the fragments, after which they disappear almost completely for randomly oriented projectiles and briefly persist ($t \lesssim 20$ fs) for aligned fragments.

III. RESULTS

To compare our calculations with the available experimental data, we have to average the stopping power ratio Eq. (6) over the time $t=D/v$, with D being the foil thickness. The average stopping power ratio is given by
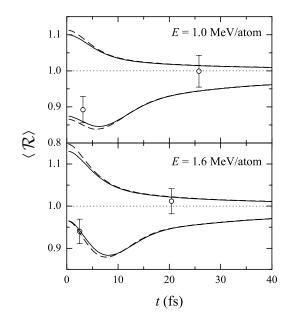
FIG. 6. Average stopping power ratio as a function of the time for O_2^+ molecular ions moving through amorphous carbon with incident energies $E = 1.0$ and 1.6 MeV/atom. Calculations considering (or not) vicinage effects in the charge state are represented by solid (or dashed) lines. The curves above unity represent $\langle \mathcal{R} \rangle$ for randomly oriented projectiles [see Eq. (7)], whereas the curves below are the corresponding ratio for projectiles moving with their interatomic axes aligned with the beam direction [see Eq. (8)]. Symbols are the experimental data for aligned projectiles [4].

$$\langle \mathcal{R} \rangle = \frac{1}{t} \int_0^t dt' \ \mathcal{R}[R_{\{ij\}}(t')], \qquad (11)$$

where $R_{\{ij\}}(t')$ are the set of interatomic distances R_{12}, R_{13}, etc., which describe the evolution with time of the cluster structure inside the target.

In Figs. 6 and 7 we present the average stopping power ratio as a function of the time, corresponding to the atomic ions resulting from the dissociation of O_2^+ and N_2^+ molecular ions, respectively, when moving through amorphous carbon foils. Symbols (and the corresponding error bars) are experimental data [4] for aligned O_2^+ or N_2^+ molecular ions. The solid lines represent our calculations taking into account the vicinage effects in the charge state, and the dashed lines show our results without considering these vicinage effects. In addition, the $\langle \mathcal{R} \rangle$ curves above 1 represent our results when the O_2^+ or N_2^+ molecular ions are randomly oriented, whereas the curves below 1 correspond to our calculations when the O_2^+ or N_2^+ molecular ions are oriented with the internuclear axis parallel to the beam direction; the latter results are those suitable for comparison with the experimental data [4]. As expected, the vicinage effects tend to disappear ($\langle \mathcal{R} \rangle \rightarrow 1$) for large times t, because the atomic ions have time enough to separate from each other, due to the screened Coulomb repulsion.

In general, our calculations reproduce the trends shown by the experimental data, i.e., $\mathcal{R} < 1$ and tending to unity as the dwell time t increases, although there is not a quantitative
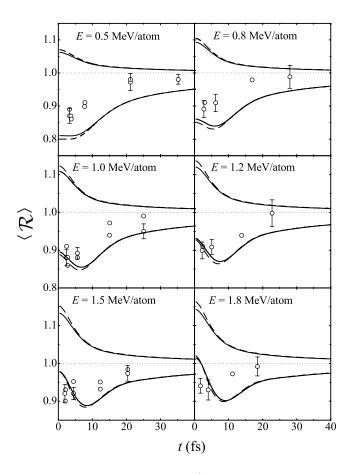

FIG. 7. Same as Fig. 6 but for N_2^+ molecular projectiles. Symbols are the experimental data for aligned projectiles [4].

agreement for all dwell times. However, the calculations corresponding to randomly oriented molecular ions always give values greater than 1 and cannot reproduce the trends of the experimental data.

It can be observed that the differences between the energy losses of these molecular ions when vicinage effects in the charge state are or are not included are almost negligible. For instance, $\mathcal{R}$ changes only by less than 1% for N_2^+ ions with $E = 0.5$ MeV/atom. In general, vicinage effects in the charge state tend to reduce the charge of the molecular fragments, which slightly decreases the vicinage effects in the energy loss of the fragments, because the interaction between the fragments is reduced as their charge state decreases.

It is worth noting that a small fraction of randomly oriented O_2^+ or N_2^+ molecular ions could contribute to the average stopping power ratio of the detected aligned fragments. Due to the alignment effect of the wake forces, that fraction increases for the larger times, and more fragments with an initially random orientation will become oriented with the internuclear axis parallel to the beam velocity. This has a net effect on the average stopping power ratio for the larger times, which contains the contribution of both aligned and random orientations. As a consequence, $\langle \mathcal{R} \rangle$ for aligned atomic ions should tend faster to unity, which would improve our present calculations.

According to Figs. 6 and 7, vicinage effects in the charge effects do not much affect the energy loss of small molecular
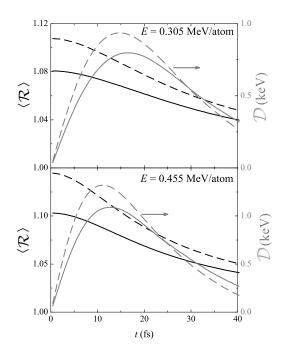
FIG. 8. Average stopping power ratio $\langle \mathcal{R} \rangle$ (left axis, black lines) and mean energy loss difference $\mathcal{D}$ (right axis, gray lines) as a function of the time, for C_{60}^+ molecular projectiles moving through amorphous carbon with incident energies $E = 0.305$ and 0.455 MeV/atom. Calculations considering (or not) vicinage effects in the charge state are represented by solid (or dashed) lines.

FIG. 9. Average stopping power ratio $\langle \mathcal{R} \rangle$ as a function of time, for C_n^+ ($n = 2$–60) molecular projectiles moving through amorphous carbon with an incident energy $E = 1$ MeV/atom. The labels over the curves indicate the number n of atoms that constitute the molecular projectile. Calculations considering (or not) vicinage effects in the charge state are represented by solid (or dashed) lines.

projectiles. However, we have found significant differences in the energy losses of larger molecular projectiles, like C_{60}^+ ions. In Fig. 8 we depict the average stopping power ratio for randomly oriented C_{60}^+ ions after traversing an amorphous carbon foil with incident energy $E = 0.305$ and 0.455 MeV/atom, which correspond to the experimental situations analyzed by Baudin *et al.* [6]. The black solid curves represent $\langle \mathcal{R} \rangle$ when vicinage effects in the charge state are considered, whereas the black dashed lines correspond to $\langle \mathcal{R} \rangle$ when these effects are not included in the calculations. In this case, $\langle \mathcal{R} \rangle > 1$ and tends to 1 as the time increases, which is a general behavior for molecular projectiles when impinging at random orientations on the target [1,3,5,6]. Note that, for instance, $\mathcal{R}$ is reduced about 4% for C_{60}^+ ions with $E = 0.455$ MeV/atom when vicinage effects in the charge state are included.

In addition to the stopping power ratio, in order to quantify vicinage effects in the energy loss, we use the difference between the mean energy loss of each molecular fragment resulting from the dissociation of the molecular projectile and that of the isolated atomic ions,

$$\mathcal{D} = \frac{\Delta E(X_n^+)}{n} - \Delta E(X^+), \qquad (12)$$

where $\Delta E(X_n^+)$ is the energy loss of the X_n^+ molecular ion and $\Delta E(X^+)$ is the energy loss of the corresponding isolated atomic ion, all incident with the same velocity. This quantity, which was used by Baudin *et al.* [6] to analyze the energy loss of swift C_{60}^+ molecular ions, is represented in Fig. 8 by
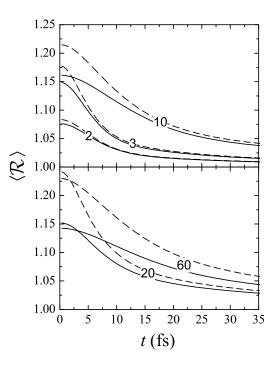
solid and dashed gray curves, depending on whether vicinage effects in the charge state were or were not included. It can be seen that $\mathcal{D} \lesssim 1$ keV (i.e., $\mathcal{D} < 1\%$ of the initial energy per atomic ion), which is in accordance with the experiments, where no energy-loss enhancement was detected within 5% of the experimental limit of observation [6].

Both $\langle \mathcal{R} \rangle$ and $\mathcal{D}$ indicate that vicinage effects in the energy loss are reduced for large clusters when the vicinage effects in the charge state are considered. This behavior could be attributed to the high packing level of the C_{60}^+ molecular ion, which makes the interaction between fragments quite strong.

In order to analyze how the packing level of the molecular projectile affects $\mathcal{R}$ through vicinage effects in the charge state, we have calculated the energy loss of C_n^+ ($n = 2$–60) ions moving through an amorphous carbon foil. These values of n cover a wide range of geometries: linear ($n = 2$) [31], ring-shaped ($n = 3, 10$) [32], and cagelike structures ($n = 20, 60$) [25,32]. We depict in Fig. 9 the stopping power ratio for C_n^+ ions with $E = 1.0$ MeV/atom in amorphous carbon. Calculations considering (or not) vicinage effects in the charge state are represented by solid (or dashed) lines; the labels on the curves indicate the number n of atoms that constitute the molecular projectile. As expected, vicinage effects in the charge state can be neglected for linear C_2^+ ions (with a reduction of $\lesssim 0.7\%$), whereas they are more important for C_3^+ and C_{10}^+ ions ($\mathcal{R}$ decreasing by $\sim 3\%$ and $\sim 5\%$, respectively, for the thinner foils), which have a ring-shaped geometrical structure. Analogously, C_{20}^+ and C_{60}^+ ions, hav-

ing cagelike structures, show a reduction in $\mathcal{R}$ even more significant ($\sim 8\%$). These results can be explained as follows. According to our model, the reduction in the charge state of the atomic ions that constitute the molecular projectile becomes more significant as the number of close neighbor atomic ions increases, which depends on the packing level of the molecular projectile. But the vicinage effects in the energy loss depend on the charge state through the interference function, Eq. (8) or (7), so a reduction in the charge state implies a decrease in the vicinage effect in the energy loss, which explains the results obtained in Fig. 9.

IV. CONCLUSIONS

The variation of the charge state of the fragments dissociated from a swift molecular ion with respect to that of the individual ions has been incorporated into the calculation of the stopping power ratio for swift molecular ions. Our calculations show that the vicinage effects in the energy loss decrease when the vicinage effects in the charge state are included. We have found that such vicinage effects are negligible for small diatomic projectiles, being noticeable only for large clusters with cagelike structures, such as C_{20}^+ and C_{60}^+. These results suggest that further experimental measurements at short dwell times could elucidate how the vicinage effects in the charge state affect the stopping power ratio.

[1] W. Brandt, A. Ratkowski, and R. H. Ritchie, Phys. Rev. Lett. **33**, 1325 (1974).

[2] P. M. Echenique, R. H. Ritchie, and W. Brandt, Phys. Rev. B **20**, 2567 (1979).

[3] J. W. Tape, W. M. Gibson, J. Remillieux, R. Laubert, and H. E. Wegner, Nucl. Instrum. Methods **132**, 75 (1976).

[4] M. F. Steuer, D. S. Gemmell, E. P. Kanter, E. A. Johnson, and B. J. Zabransky, Nucl. Instrum. Methods Phys. Res. **194**, 277 (1982).

[5] K. Narumi, K. Nakajima, K. Kimura, M. Mannami, Y. Saitoh, S. Yamamoto, Y. Aoki, and H. Naramoto, Nucl. Instrum. Methods Phys. Res. B **135**, 77 (1998).

[6] K. Baudin, A. Brunelle, M. Chabot, S. Della-Negra, J. Depauw, D. Gardès, P. Håkansson, Y. Le Beyec, A. Billebaud, M. Fallavier, J. Remillieux, J. C. Poizat, and J. P. Thomas, Nucl. Instrum. Methods Phys. Res. B **94**, 341 (1994).

[7] J. Jensen and P. Sigmund, Phys. Rev. A **61**, 032903 (2000).

[8] S. Heredia-Avalos, R. Garcia-Molina, and I. Abril, Nucl. Instrum. Methods Phys. Res. B **164-165**, 296 (2000).

[9] S. Heredia-Avalos and R. Garcia-Molina, Phys. Lett. A **275**, 73 (2000).

[10] Y.-N. Wang, H.-T. Qiu, and Z. L. Mišković, Phys. Rev. Lett. **85**, 1448 (2000).

[11] Z. L. Mišković, S. G. Davison, F. O. Goodman, W.-K. Liu, and Y.-N. Wang, Phys. Rev. A **63**, 022901 (2001).

[12] R. Garcia-Molina and S. Heredia-Avalos, Phys. Rev. A **63**, 044901 (2001).

[13] S. Heredia-Avalos, C. D. Denton, R. Garcia-Molina, and I. Abril, Phys. Rev. Lett. **88**, 079601 (2002).

[14] E. Nardi, Z. Zinamon, T. A. Tombrello, and N. M. Tanushev, Phys. Rev. A **66**, 013201 (2002).

[15] L. Lammich, H. Buhr, H. Kreckel, S. Krohn, M. Lange, D. Schwalm, R. Wester, A. Wolf, D. Strasser, D. Zajfman, Z. Vager, I. Abril, S. Heredia-Avalos, and R. Garcia-Molina, Phys. Rev. A **69**, 062904 (2004).

[16] A. Chiba, Y. Saitoh, and S. Tajima, Nucl. Instrum. Methods Phys. Res. B **232**, 32 (2005).

[17] N. R. Arista, Nucl. Instrum. Methods Phys. Res. B **164-165**, 108 (2000).

[18] Z. L. Mišković, Y.-N. Wang, and Y.-H. Song, Nucl. Instrum. Methods Phys. Res. B **256**, 57 (2007).

[19] D. Maor, P. J. Cooney, A. Faibis, E. P. Kanter, W. Koenig, and B. J. Zabransky, Phys. Rev. A **32**, 105 (1985).

[20] A. Brunelle, S. Della-Negra, J. Depauw, D. Jacquet, Y. Le Beyec, and M. Pautrat, Phys. Rev. A **59**, 4456 (1999).

[21] S. Heredia-Avalos, R. Garcia-Molina, and N. R. Arista, Europhys. Lett. **54**, 729 (2001).

[22] J. F. Ziegler, J. P. Biersack, and U. Littmark, *The Stopping and Range of Ions in Solids* (Pergamon, New York, 1985), Vol. 1.

[23] W. Brandt and M. Kitagawa, Phys. Rev. B **25**, 5631 (1982).

[24] K. P. Huber, in *American Institute of Physics Handbook*, edited by B. H. Billins, H. P. R. Frederikse, D. F. Bleil, R. B. Lindsay, R. K. Cook, J. B. Marion, H. M. Crosswhite, and M. W. Zemansky, coordinating editor D. E. Gray (McGraw-Hill, New York, 1972), pp. 7–168.

[25] J. K. Labanowskiin and I. Filippov, http://server.ccl.net/

[26] N. R. Arista, Phys. Rev. B **18**, 1 (1978).

[27] I. Abril, R. Garcia-Molina, C. D. Denton, F. J. Pérez-Pérez, and N. R. Arista, Phys. Rev. A **58**, 357 (1998).

[28] S. Heredia-Avalos, R. Garcia-Molina, J. M. Fernández-Varea, and I. Abril, Phys. Rev. A **72**, 052902 (2005).

[29] P. Sigmund, *Stopping of Heavy Ions* (Springer, Berlin, 2004).

[30] C. C. Montanari and J. E. Miraglia, Phys. Rev. A **73**, 024901 (2006).

[31] J. D. Watts and R. J. Bartlett, J. Chem. Phys. **96**, 6073 (1992).

[32] A. Van Orden and R. J. Saykally, Chem. Rev. **98**, 2313 (1998).